PERGAMON

International Journal of Heat and Mass Transfer 42 (1999) 3599–3608

International Journal of HEAT and MASS TRANSFER

www.elsevier.com/locate/ijhmt

Boundary layer flows in a vertical porous enclosure induced by opposing buoyancy forces

A. Amahmid[a], M. Hasnaoui[a], M. Mamou[b], P. Vasseur[b,*]

[a]*Département de Physique, Faculté des Sciences Semlalia, Marrakech, B.P. S-15, Maroc*
[b]*Ecole Polytechnique, C.P. 6079, Suc. 'Centre-Ville', Montreal, P.Q., Canada H3C 3A7*

Received 3 August 1998; received in revised form 4 January 1999

Abstract

Double diffusive natural convection induced in a vertical porous layer subject to opposing horizontal gradients of heat and mass is studied analytically and numerically using the Darcy model with the Boussinesq approximation. The governing parameters for the problem are the thermal Rayleigh number, R_T, the Lewis number, Le, the buoyancy ratio, N and the aspect ratio, A, of the enclosure. The analytical solution is developed on the basis of the parallel flow approximation. A numerical study is performed to validate the results of the analytical predictions. It is demonstrated in this study that there exists a domain in (Le, N) plane where, at large R_T, boundary layer profiles are obtained for the velocity and density but not for the temperature and concentration. The boundary layer regimes obtained for this domain ($N < 0$) are extremely different from those found in the previous studies for the case of aiding buoyancy forces ($N > 0$).

1. Introduction

Double diffusive natural convection induced in a fluid-saturated porous medium is widely encountered in nature and technological processes. The engineering applications of the problem are of importance in many situations like the migration of moisture through air contained in fibrous insulations, food processing, contaminant transport in ground water, electrochemical processes, etc. While considerable research has been carried out on thermally driven natural convection in porous media (see for instance Nield and Bejan [1]), relatively less work has been done on natural convection due to combined buoyancy forces. The aim of the present study is to discuss a boundary layer solution for free convection, within a rectangular cavity, due to opposing buoyancy effects ($N < 0$).

Past studies on double diffusive convection in a vertical porous enclosure indicate that the resulting flows can be very different from those driven by the temperature field solely, especially when the buoyancy forces are opposing each other. For instance, for the case of opposing and equal buoyancy forces ($N = -1$) the rest state, in a vertical cavity with constant temperature and concentration on the vertical walls, is an exact solution of the problem. The stability of this solution was investigated by Charrier-Mojtabi et al. [2] on the basis of the linear stability theory. The critical Rayleigh number, for the onset of supercritical convection, was derived by these authors in terms of the aspect ratio A of the cavity and the Lewis number Le. Their results were extended by Mamou et al. [3] to consider the case of an inclined cavity. It was demonstrated that for values of Lewis number around unity, overstability is possible, provided that the normalized porosity of the

* Corresponding author. Tel.: +1-514-340-4711; fax: +1-514-340-5917.
E-mail address: vasseur@meca.polymtl.ca (P. Vasseur)

0017-9310/99/$ - see front matter
PII: S0017-9310(99)00019-8

Nomenclature

A	aspect ratio of the enclosure, H'/L'
D	mass diffusivity of species
g	gravitational acceleration
H'	height of the enclosure
j'	constant mass flux per unit area
K	permeability of the porous medium
L'	thickness of the enclosure
Le	Lewis number, α/D
N	buoyancy ratio, $\beta_S\Delta S'/\beta_T\Delta T'$
Nu	Nusselt number, Eq. (7)
q'	constant heat flux per unit area
R_T	thermal Darcy–Rayleigh number, $g\beta_T Kq'L'^2/(\lambda\alpha\nu)$
S	dimensionless concentration, $(S'-S'_0)/\Delta S'$
Sh	Sherwood number, Eq. (7)
S'_0	reference concentration
$\Delta S'$	characteristic concentration, $j'L'/D$
t	dimensionless time, $t'\alpha/(L'^2\sigma)$
T	dimensionless temperature, $(T'-T'_0)/\Delta T'$
T'_0	reference temperature
$\Delta T'$	characteristic temperature, $q'L'/\lambda$
(u, v)	dimensionless velocities in (x, y) directions, $(u'L'/\alpha, v'L/\alpha)$
(x, y)	dimensionless coordinates axis, $(x'/L', y'/L')$

Greek symbols

α	thermal diffusivity
β_S	concentration expansion coefficient
β_T	thermal expansion coefficient
ε	normalized porosity, ϵ/σ
ϵ	porosity of the porous medium
λ	thermal conductivity
ν	kinematic viscosity of the fluid
ρ	density of the fluid mixture
ρ_a	dimensionless density of the fluid, $-(T+NS)$
$(\rho c)_f$	heat capacity of fluid mixture
$(\rho c)_p$	heat capacity of saturated porous medium
σ	heat capacity ratio, $(\rho c)_p/(\rho c)_f$
Ψ	dimensionless stream function, Ψ'/α
ζ	dimensionless vorticity, $\zeta'L'^2/\alpha$
η	inertial parameter, $(C_aK\alpha)/(\sigma L'\nu)$

Superscript

$'$	dimensional variable

Subscripts

max	maximum value
min	minimum value
0	reference state
S	solutal
T	thermal

porous medium is made smaller than unity. The case of a vertical cavity with constant gradients of temperature and concentration prescribed on the vertical walls of the enclosure has been considered by Mamou et al. [4]. A linear stability was carried out to describe the oscillatory and the stationary instability in terms of the governing parameters of the problem. By using the parallel flow approximation it was demonstrated that there exists a subcritical Rayleigh number at which a stable convective solution bifurcates from the rest state through finite amplitude convection. The effect of the Darcy number on the subcritical Rayleigh number was investigated analytically and numerically by Amahmid et al. [5]. Their results were found to reduce to the regular Darcy's law and viscous flows solution in the limits of low and high porosities, respectively.

A limited number of investigations concerning double diffusive natural convection in rectangular porous enclosures, induced by opposing buoyancy effects, have been reported in the literature. Trevisan and Bejan [6] used numerical methods to study heat and mass convection in a square cavity subjected to heat and mass gradients in the horizontal direction. They observed that the Nusselt and Sherwood numbers were minimum in the vicinity of $N=-1$. Similar results have been reported by Lin [7], Alavyoon et al. [8], Mamou et al. [9] and Nithiarasu et al. [10] for a variety of boundary conditions. It was demonstrated numerically by Alavyoon et al. [8] that there is a domain of N (<0) in which oscillating convection is obtained for a given set of the governing parameters. Outside this domain, the solution approaches steady-state convection. Also, for opposing forces, the existence of multiple solutions has been demonstrated analytically and numerically by Mamou et al. [9] and [11] and Amahmid et al. [12]. For a given value of N, it was demonstrated in Ref. [11] that both Lewis and Rayleigh numbers have an influence on the domain of existence of these multiple steady state solutions.

The objective of the analytical and numerical work of the present study is to discuss the existence of boundary layer flows induced by opposing buoyancy effects in a vertical slot. Boundary layer analyses have been used in the past by Trevisan and Bejan [6] and [13], Alavyoon [14] and Mamou et al. [9], among others, to study the natural convective flows due to the combined thermal and species diffusion effects. In general, boundary layer models are expected to be invalid when the two buoyant mechanisms oppose each other, and are of the same order. However, it is demonstrated in this investigation that there exists a domain of the Lewis number and the buoyancy ratio N ($N<0$) in which boundary layer solutions are possible for large Rayleigh numbers.

In the following, the mathematical model and the solution procedure are discussed. The results presented here are relevant to a better understanding of double diffusive flows in porous media.

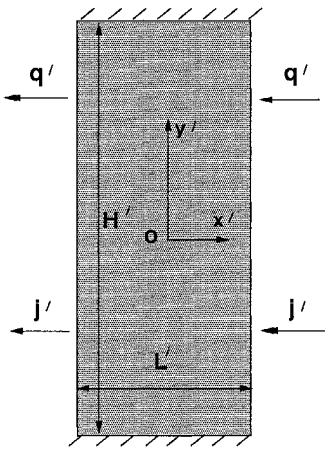

Fig. 1. Schematic diagram of the studied system.

2. Mathematical model

The studied configuration is a two dimensional rectangular porous matrix of height H' and width L'. The geometry of the enclosure is sketched in Fig. 1. The vertical sides of the enclosure are subjected to constant fluxes of heat q' and mass j' while its horizontal sides are isolated. The fluid saturated porous medium is assumed isotropic and homogeneous and the Darcy model is considered. Using the Boussinesq approximation and assuming constant properties, the dimensionless equations governing this problem are:

$$\eta\frac{\partial\zeta}{\partial t}+\zeta=R_{\mathrm{T}}\left(\frac{\partial T}{\partial x}+N\frac{\partial S}{\partial x}\right) \tag{1}$$

$$\nabla^2\Psi=-\zeta \tag{2}$$

$$\frac{\partial T}{\partial t}+u\frac{\partial T}{\partial x}+v\frac{\partial T}{\partial y}=\nabla^2 T \tag{3}$$

$$\epsilon\frac{\partial S}{\partial t}+u\frac{\partial S}{\partial x}+v\frac{\partial S}{\partial y}=\frac{1}{Le}\nabla^2 S \tag{4}$$

The velocity profiles are related to the stream function by

$$u=\frac{\partial\Psi}{\partial y};\quad v=-\frac{\partial\Psi}{\partial x} \tag{5}$$

where ζ, Ψ, T and S are the dimensionless vorticity, stream function, temperature and concentration, re-

spectively. The parameter R_T is the thermal Rayleigh number, N the buoyancy ratio and Le the Lewis number. The constant η is given by $\eta=(C_aK\alpha)/(\sigma L'\nu)$, where C_a is an acceleration coefficient [1]. Preliminary tests have indicated that an adequate choice of the parameter η, used here as a relaxation factor in the numerical method, reduces considerably the computation time.

The boundary conditions for Eqs. (1)–(5) are:

$$\Psi=0;\quad \partial T/\partial x=\partial S/\partial x=1 \quad \text{for} \quad |x|=1/2$$

$$\Psi=\partial T/\partial y=\partial S/\partial y=0 \quad \text{for} \quad |y|=A/2 \tag{6}$$

The heat and mass transfer rates are of interest in many engineering applications. They are evaluated in terms of the Nusselt and Sherwood numbers which are given respectively by:

$$Nu=\frac{1}{T_{(\frac{1}{2},0)}-T_{(-\frac{1}{2},0)}},$$
$$Sh=\frac{1}{S_{(\frac{1}{2},0)}-S_{(-\frac{1}{2},0)}} \tag{7}$$

Note that, according to the boundary conditions (Eqs. (6)), the thermal buoyancy forces tend to induce a counterclockwise fluid circulation while the solutal buoyancy forces tend to induce a clockwise fluid circulation for $N<0$ (case of opposing flows) and a counterclockwise fluid circulation for $N>0$ (case of cooperative flows).

3. Numerical method

The governing equations are discretized according to the central finite difference scheme. The iterative procedure is performed using the alternate direction implicit method (ADI). The streamfunction field is determined from Eq. (2) using the successive over relaxation method (SOR). The calculation domain was divided into three regions in the horizontal direction (x-direction). For the two regions adjacent to the vertical walls where the horizontal gradients are important (boundary layer regions) a uniform fine grid was used while a coarse uniform grid was employed for the central region of the cavity. First order accurate discretization was used in the interface between two different grids. In some situations, this procedure was also applied to the y-direction to refine the grid in the vicinity of the horizontal walls. At high R_T and A, the central difference scheme caused numerical instabilities in a few cases among those considered in this study. The problem was solved in these particular situations by using a second upwind differencing scheme [15] to discretize the temperature and concentration equations.

4. Analytical solution

For large aspect ratio ($A\gg1$) it has been demonstrated in the past by several authors [5,9,12,14] that the present problem can be significantly simplified by the approximation of the parallel flow. With this approximation $u=0$ and $v=v(x)$ in the central part of the cavity, i.e. outside the end regions. The approximation allows the following simplifications:

$$\Psi(x,y)=\Psi(x)$$

$$T(x,y)=C_Ty+\theta_T(x)$$

$$S(x,y)=C_Sy+\theta_S(x) \tag{8}$$

where C_T and C_S are unknown temperature and concentration gradients respectively in the y-direction. Those gradients are determined by imposing zero heat and mass transfer across any transversal section of the cavity.

Introducing these approximations into the steady state form of Eqs. (1)–(4) and solving the resulting equations, together with the boundary conditions (6), it is found (see for instance Refs. [9] and [14]) that the solution depends on the sign of the parameter Ω^2, defined as

$$\Omega^2=R_T(NLeC_S+C_T) \tag{9}$$

Of particular interest is the boundary layer flow regime for which it is possible to simplify the resulting solution. In the following discussion it is assumed that $\Omega^2>0$, since only positive values of this parameter can lead to boundary layer behaviors. It can be easily shown that, for $x>0$, the boundary layer regime ($\Omega\gg1$) is described by the following equations:

$$\Psi(x)=a[1-e^{\Omega(x-1/2)}];\quad v=a\Omega e^{\Omega(x-1/2)} \tag{10}$$

$$T=C_Ty+(1-aC_T)x+\frac{aC_T}{\Omega}e^{\Omega(x-1/2)} \tag{11}$$

$$S=C_Sy+(1-aLeC_S)x+\frac{aLeC_S}{\Omega}e^{\Omega(x-1/2)} \tag{12}$$

where $a=R_T(N+1)/\Omega^2$ and

$$C_T=\frac{a(1-2/\Omega)}{1+G(1-3/\Omega)};\quad C_S=\frac{aLe(1-2/\Omega)}{1+Le^2G(1-3/\Omega)} \tag{13}$$

Substituting Eqs. (11) and (12) into Eqs. (7) yields the

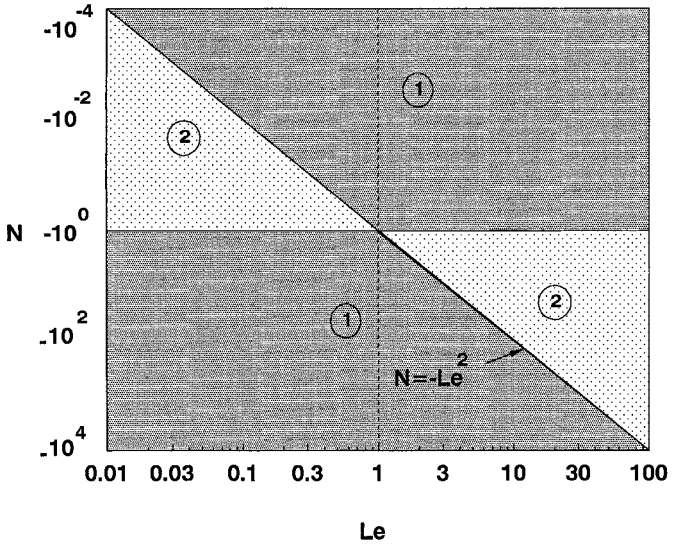

Fig. 2. Domains corresponding to different boundary layer regimes.

following expressions for the Nusselt and Sherwood numbers

$$Nu = \frac{1 + G(1 - 3/\Omega)}{1 + G(1 - 4/\Omega)/\Omega};$$
$$Sh = \frac{1 + Le^2 G(1 - 3/\Omega)}{1 + Le^2 G(1 - 4/\Omega)/\Omega} \tag{14}$$

In the above equations, G is given by

$$G = a^2 = \frac{\Omega}{2C_1}\left(C_2 \pm \sqrt{C_2^2 + C_3}\right) \tag{15}$$

where $C_1 = Le^2(\Omega - 3)(N+1)$, $C_2 = (\Omega - 3)(N + Le^2) - 1 - NLe^2$ and $C_3 = 4C_1(N+1)$. It is noted that since $G > 0$ and $C_3 > 0$, it follows that only one of the two relations of Eq. (15) is to be considered (the choice of which depends on the sign of C_1).

The parameter Ω is a measure of the inverse of the thickness of the vertical boundary layer ($\delta \sim 1/\Omega$). For sufficiently large values of this parameter ($\Omega \gg 1$), Eq. (15) reduces to

$$G = d_1\Omega \quad \text{if} \quad d_1 > 0 \tag{16}$$

and

$$G = \frac{-1}{d_1 Le^2} = \frac{-(1+N)}{(N + Le^2)} \quad \text{if} \quad d_1 < 0 \tag{17}$$

where $d_1 = (1 + N/Le^2)/(1+N)$.

The solution corresponding to Eq. (16) has been largely discussed in the past. The purpose of the present study is to point out the particularity of the solutions predicted by Eq. (17). It is to be noted that this type of solution is possible only in the case of opposing flows ($N < 0$) and requires the following condition:

$$-\max(1, Le^2) < N < -\min(1, Le^2) \tag{18}$$

The domains where these conditions are satisfied are delineated in Fig. 2. They correspond to region 2 in the (Le, N) plane. For this situation, when R_T is sufficiently large, Ω is given, according to Eq. (17), by

$$\Omega = R_T^{1/2} \mid (1+N)(N + Le^2) \mid^{1/4} \tag{19}$$

4.1. Effect of R_T

In this section the effect of R_T will be discussed for given values of N and Le. For the boundary layer flow regime corresponding to the case of $d_1 > 0$, it has been demonstrated in Refs. [9] and [14] that Ω and G vary as $R_T^{2/5}$, the maximum velocity $v(x = 1/2)$ varies as $R_T^{3/5}$ and the flow intensity $\Psi_0 = |\Psi(x = 0)|$ varies as $R_T^{1/5}$. As a result, at high values of R_T, Nu and Sh vary as $R_T^{2/5}$, C_T and C_S vary as $R_T^{-1/5}$ and the vertical gradients of both T and S are nearly zero in the cavity. In addition, the horizontal gradients of both T and S are also nearly zero outside a very thin layer adjacent to the vertical boundaries. This implies that the horizontal profiles of T and S exhibit the boundary layer behavior. Furthermore, the increase of R_T tends to make uniform the temperature and concentration (and thereby the density) in the core region of the enclosure.

The above results are fundamentally different for the case $d_1 < 0$ and large R_T as it will be discussed now. For this situation, Ω and $v(x = 1/2)$ vary as $R_T^{1/2}$ and

consequently, G and thereby Ψ_0, C_T, C_S, Nu and Sh become independent of R_T. At this stage it is convenient to introduce the parameter ρ_a which characterizes the dimensionless density of the binary fluid as

$$\rho_a = -(T+NS)$$

$$= -(C_T + NC_S)y - \frac{(1+N)}{\Omega} e^{\Omega(x-1/2)} \quad (20)$$

as predicted by Eqs. (11)–(13) and (17).

The above equation clearly shows that, at large R_T, the horizontal gradient of the density $(\partial\rho_a/\partial x)$ becomes zero in the core region while the vertical gradient of the density $(\partial\rho_a/\partial y)$ becomes constant and is given by

$$\frac{\partial\rho_a}{\partial y} = \frac{-[-(1-N)(N+Le^2)]^{1/2}}{Le+1} \quad (21)$$

Furthermore, if $Le \gg 1$ and $Le^2 \gg |N|$, this above gradient corresponding to $R_T \to \infty$ can be related to the horizontal gradient of the diffusive regime ($R_T = 0$) by:

$$\left[\frac{\partial\rho_a}{\partial y}\right]_{R_T\to\infty} = -\sqrt{-(1+N)} = -\sqrt{\left[\frac{\partial\rho_a}{\partial x}\right]_{R_T=0}}$$

$$= 0 \quad (22)$$

In other words, this means that for this case, the convective boundary layer flow makes zero the horizontal gradient obtained for the diffusive regime and creates a vertical gradient of the density equal to the square root of the horizontal diffusive one. This behavior is qualitatively similar to that obtained at large R_T in the case of a rectangular cavity with vertical walls maintained at different constant temperatures where the thermal natural convection tends to make zero the horizontal gradient of the temperature (and thereby that of the density) in the core region and imposes a vertical stratification which is not existing in the diffusive regime. It can be easily verified that for $d_1 > 0$, both horizontal and vertical gradients of the density are zero at large R_T.

For the case of $d_1 < 0$, it is readily found from Eqs. (14) and (17) that the parameters Nu, Sh and Ψ_0 tend towards the following constant values as $R_T \to \infty$:

$$Nu \to \frac{Le^2-1}{N+Le^2}, \quad Sh \to -NNu, \quad \Psi_0 \to \sqrt{G} \quad (23)$$

while the temperature and concentration distributions become linear if we except the immediate vicinity of the vertical boundaries. They are expressed as:

$$T = C_T y + \frac{x}{Nu} \quad \text{and} \quad S = C_S y + \frac{x}{Sh} \quad (24)$$

Furthermore, when the condition $Le^2 \gg |N| > 1$ is satisfied, Nu, Sh and Ψ_0 reduce to

$$Nu \simeq 1, \quad Sh = -N \quad \text{and} \quad \Psi_0 = \sqrt{-(1+N)/Le^2} \quad (25)$$

and the horizontal gradients of T and S in the core region are given by:

$$\frac{\partial T}{\partial x} \simeq 1 \quad \text{and} \quad \frac{\partial S}{\partial x} \simeq -\frac{1}{N} \quad (26)$$

This implies that the temperature profile is identical to the one corresponding to the diffusive regime. In addition, if the value of $|N|$ is of order of unity, the concentration gradient in the core region is of the same order as that in the immediate vicinity of the vertical boundaries (where $\partial S/\partial x = 1$) and it becomes obvious in this case that the temperature and the concentration profiles have not got the characteristics of the boundary layer profiles. Nevertheless, these profiles are such that their combination in the relation $\rho_a = -(T+NS)$ leads to boundary layer profiles for the density. In fact it is clear from Eq. (26) that the horizontal gradient of the density $(\partial\rho_a/\partial x)$ is zero in the core region at large R_T. Note that the diffusive transfers of heat and mass in this case are of non-negligible importance even at very large R_T. The linear expressions obtained in Eq. (24) also indicate that the contour lines of the temperature and concentration consist of straight lines tilted with respect to the vertical direction. This result can be clearly observed on the contour lines reported in Ref. [9] for $R_T = 50$, $Le = 10$ and $N = -1.8$. The inclination angles (with respect to the vertical direction) of the temperature and concentration contour lines denoted respectively by φ_T and φ_S, and the gradients of these two quantities in the normal direction to the contours (outside a very thin layer adjacent to the vertical boundary) are given by

$$\cos(\varphi_T) = \frac{\partial T}{\partial n_T} = \frac{1}{\sqrt{Nu}}$$

$$\cos(\varphi_S) = \frac{\partial S}{\partial n_S} = \frac{1}{\sqrt{Sh}} \quad (27)$$

where n_T and n_S are the normals to the contour lines of the temperature and concentration respectively. In the case of $Le^2 \gg |N| > 1$, φ_T and φ_S verify:

$$\cos(\varphi_T) = 1 \quad \text{and} \cos(\varphi_S) = \frac{1}{\sqrt{-N}} \quad (28)$$

which means that the isotherms are vertical ($\varphi_T = 0$) and the inclination angle for the concentration lines is higher (the upper limit is $\pi/2$) at higher values of $-N$.

The inclinations are in clockwise and counterclockwise directions respectively for $N < -1$ and $N > -1$. The relations (27) show that the characteristics of the

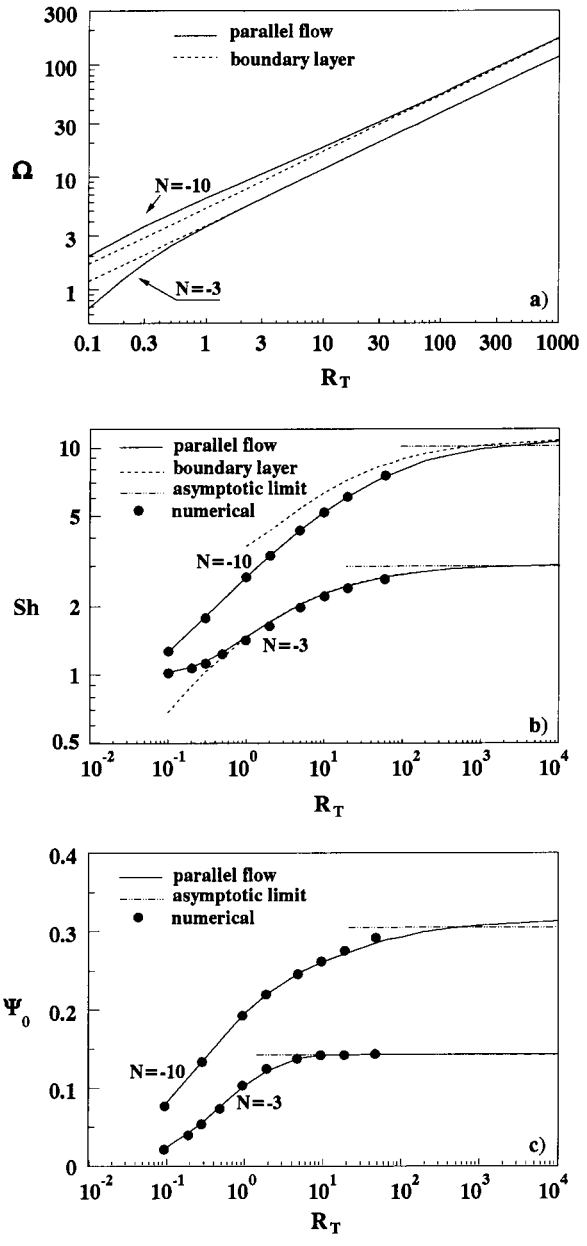

Fig. 3. Rayleigh number effect, R_T, on: (a) Ω, (b) *Sh* and (c) Ψ_0 for $Le=10$ and $N=-3$ and -10.

heat and mass transfers, namely *Nu* and *Sh*, and thereby the importance of the convective effects can be determined by simply measuring the inclination angles of the isotherms and isosolutes with respect to the vertical direction.

The behaviors obtained for the boundary layer flows when $d_1 < 0$ are illustrated in Fig. 3a–c where Ω, *Sh* and Ψ_0 evolutions with R_T are presented for $Le=10$, $N=-3$ and -10. It can be seen that the exact analytical solution (solid lines) based on the parallel flow hypothesis [9,12] agrees well with the numerical results obtained by solving the full governing equations. The boundary layer analytical approximations (14) and (19) (dotted lines) are seen in good agreement with the exact solution at relatively (depending on N) large R_T. The agreement is obtained for $R_T>1$ and $R_T>100$ respectively for $N=-3$ and $N=-10$. The quantities *Sh* and Ψ_0 are observed to reach asymptotic variations predicted by Eq. (25) at large R_T. The Nusselt number has also an asymptotic evolution with R_T and it is well predicted by the boundary layer approximate solutions but it is not presented here since its values remain always close to unity ($Nu \leqslant 1.1$) which means that the heat transfer is always dominated by the diffusive effect in this case even at very large R_T. This is due to the relatively large value of *Le* ($Le=10$) considered in this case. Also the diffusive mass transfer is not negligible at large R_T in the case of $N=-3$ since the asymptotic value of *Sh* is approximately equal to three times the value of the pure diffusion ($Sh \simeq 3.02$).

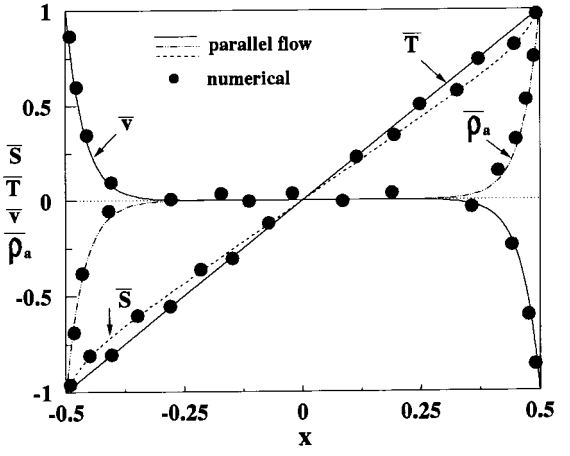

Fig. 4. Horizontal profiles of: velocity; temperature; concentration; and density for $A=6$, $Le=10$, $N=-3$ and $R_T=50$.

Fig. 4 illustrates the horizontal profiles of velocity, $\bar{v}=v/v_{max}$, temperature, $\bar{T}=T/T_{max}$, concentration $\bar{S}=S/S_{max}$, and density, $\overline{\rho_a}=\rho_a/\rho_{a\,max}$, at mid-height ($y=0$) of the enclosure for $R_T=50$, $Le=10$ and $N=-3$. The subscript max refers to maximum values of v, T, S and ρ_a obtained at $y=0$. It can be seen that the numerical results are in good agreement with the exact analytical solution. Furthermore, it is noted that the temperature and concentration profiles are not of boundary layer type although the velocity and the density profiles are so. In fact, the density and velocity gradients are nearly zero in the core region while the temperature and the concentration gradients are important in this region. This also confirms the fact that the diffusive transfer is of non-negligible importance

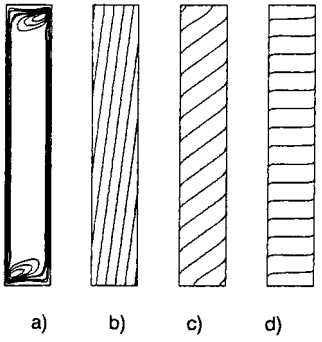

Fig. 5. Contour lines of: (a) stream function; (b) temperature; (c) concentration; and (d) density for $A=6$, $Le=10$, $N=-3$ and $R_T=50$.

even at large values of R_T. The contour lines for the stream function, the temperature, the concentration and the density are presented in Fig. 5 for $R_T=50$, $Le=10$ and $N=-3$. The flow is parallel to the vertical walls in the core region and small recirculating cells are induced in the vicinity of the horizontal boundaries. The isotherms and isosolutes are nearly straight lines tilted with respect to the vertical direction. The tilt angle corresponding to the isotherms is smaller than that corresponding to the isosolutes since the temperature field is more influenced by the diffusive effect ($Le>1$). The tilt angles φ_T and φ_S deduced from the numerical results are about 7.7° and 54° respectively. Such values are close to those predicted by the analytical relations (27) namely 8.17° and 55.1° corresponding to infinite R_T. Fig. 5 shows also that the boundary layer flow makes zero the horizontal gradient of the density in the core region. The vertical stratification observed indicates that the vertical density gradient is not eliminated and the boundary layer flow does not tend to make uniform the density in the enclosure as is the case with the boundary layer flows corresponding to the case $d_1>0$. The vertical density gradient obtained numerically for $R_T=50$, $Le=10$ and $N=-3$ ($\partial\rho_a/\partial y\simeq-1.21$) is found to be close to the value given by Eq. (21) ($\partial\rho_a/\partial y\simeq-1.27$).

4.2. Effect of Le

When R_T and N ($N<-1$) are maintained constant, Eq. (19) (which is valid only for $Le>\sqrt{-N}$) indicates that Ω increases monotonically with Le. At large Le, Ω can be expressed as:

$$\Omega=(R_T Le)^{1/2}\mid N+1\mid^{1/4}=R_S^{1/2}\frac{\mid N+1\mid^{1/4}}{\mid N\mid^{1/2}} \tag{29}$$

where $R_S=(R_T|N|Le)$ is the solutal Rayleigh number.

Relations (22) show that Nu and Sh have asymptotic values: $Nu\to 1$ and $Sh\to -N$. These limits are independent of R_T and indicate that the heat transfer is dominated by diffusion effects at large Le independently of R_T. Also, it is seen from Eq. (29) that the quantity Ω varies as $R_S^{1/2}$. Yet, these behaviors are different from those observed for $d_1>0$. In fact, the results obtained by Mamou et al. [9] clearly show that for fixed R_T and N ($N>-1$), Ω becomes independent of Le at large values of this parameter and Nu and Sh

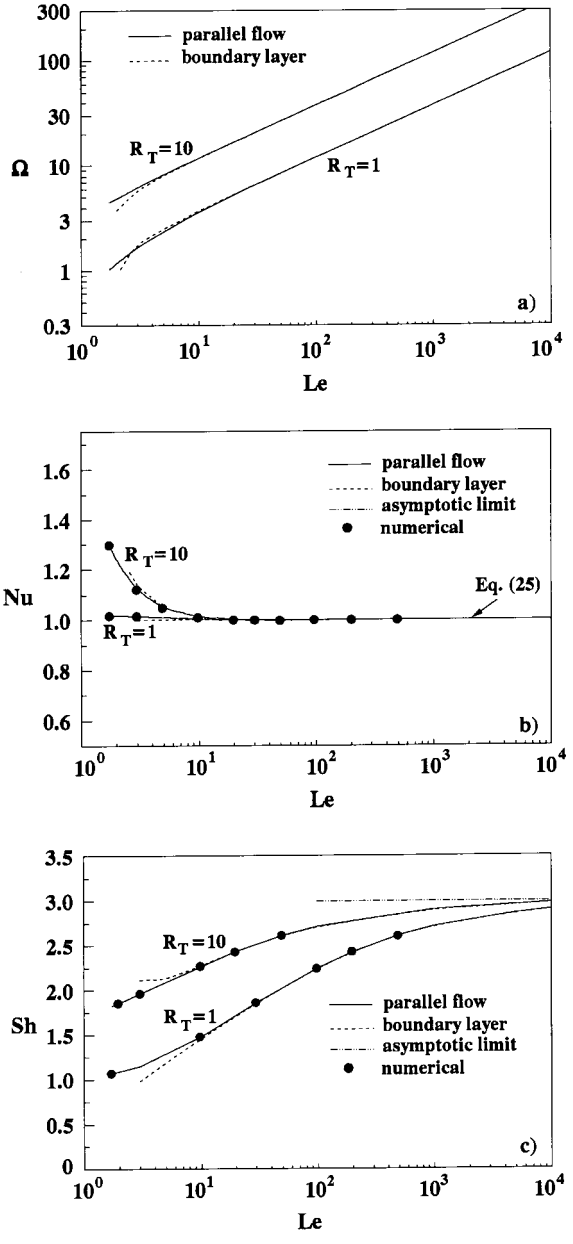

Fig. 6. Variations with Le for $N=-3$, and $R_T=1$ and 10: (a) Ω variations; (b) Nu variations; and (c) Sh variations.

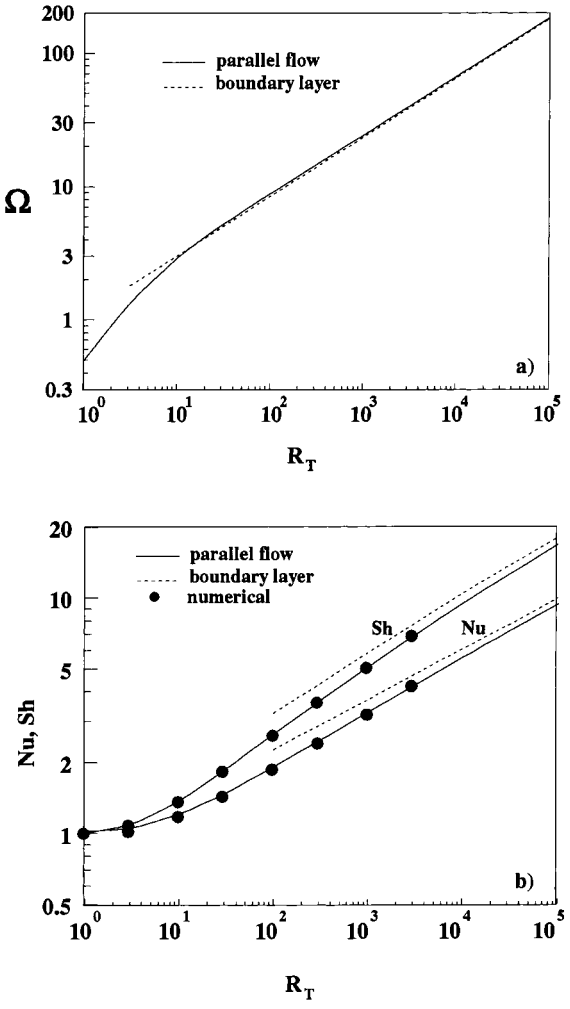

Fig. 7. Variations with R_T for $N=-2$ and $Le=\sqrt{2}$: (a) Ω variations; (b) *Nu* and *Sh* variations.

also tend towards asymptotic values at large *Le*. However, these values depend on R_T and the asymptotic heat and mass transfers (obtained at large *Le*) may be dominated by convection when R_T is large enough. The effect of *Le* on the quantities Ω, *Nu* and *Sh* is illustrated in Fig. 6a–c for $N=-3$, $R_T=1$ and 10. It is seen from Fig. 6a that Ω increases monotonically with *Le* and the analytical exact solution is well predicted by the approximate relations (14) and (19) for $Le>10$. Also *Nu* and *Sh* exhibit asymptotic behaviors with *Le* and tend to become independent of R_T at large *Le*.

Another type of boundary layer regime is obtained for the particular case where $N+Le^2=0$ (i.e. $N=-Le^2$). For this situation, $C_1=Le^2(\Omega-3)(1-Le^2)$, $C_2=-(1-Le^4)$ and $C_3=4C_1(1-Le^2)$. If *Le* (and thereby *N*) is maintained constant and R_T and Ω are sufficiently large, then Eq. (15) yields

$$G=\frac{\Omega}{Le(\Omega-3)^{1/2}} \tag{30}$$

where

$$\Omega=R_T^{4/9}[(1-Le^2)^2Le]^{2/9} \tag{31}$$

At very large values of R_T, *Nu* and *Sh* (Eqs. (14)) reduce to

$$Nu=\frac{\Omega^{1/2}}{Le} \quad Sh=Le\Omega^{1/2}=Le^2Nu \tag{32}$$

It is clear that for this particular situation, Ω varies as $R_T^{4/9}$ and *Nu* and *Sh* varies as $R_T^{2/9}$. The corresponding variations of Ω, *Nu* and *Sh* with R_T are illustrated in Fig. 7a and b for $N=-Le^2=-2$. It can be seen from Fig. 7a that for $R_T>10$, the approximate solution of Ω (Eq. (31)) coincides with the exact one. For *Nu* and *Sh*, the approximate solutions are based on Eqs. (14), (30) and (31). It can be seen from Fig. 7b that they (approximate solutions) are close to the exact solutions at large R_T.

The domains corresponding to the different boundary layer flows that may be encountered in this problem are presented in Fig. 2. For region 1 (and for aiding flows: $N>0$) Ω varies as $R_T^{2/5}$. For region 2, Ω varies as $R_T^{1/2}$. For the curve $N=-Le^2$, Ω varies as $R_T^{4/9}$. For $N=-1$ there is no boundary layer flow since convective solutions corresponding to $\Omega^2>0$ are not possible in this case. This situation has been discussed in details in Refs. [2–4].

5. Conclusion

Double diffusive natural convection is studied analytically and numerically in a vertical porous layer submitted to constant fluxes of heat and mass on its vertical sides. It is demonstrated in the case of opposing flows that there exists a domain in the (*Le*, *N*) plane where a boundary layer regime can be observed for the velocity and density profiles even though neither the temperature nor the concentration profiles exhibit such a behavior. The boundary layer thickness for the resulting flow varies as $R_T^{-1/2}$. Linear distributions are obtained for the temperature and concentration at large R_T and *Nu* and *Sh* exhibit asymptotic evolutions with this parameter. In particular, it is demonstrated that $Nu\rightarrow 1$, $Sh\rightarrow -N$ and $\Psi_0\rightarrow Le|N+1|^{1/2}$ when the condition $Le^2\gg|N|>1$ is satisfied. Furthermore, the diffusive heat and mass transfers can be of non-negligible importance even at very large values of R_T. Also for given R_T and $N<-1$ and for sufficiently large *Le* such that $(Le^2+N)(1+N)<0$, the heat and mass transfers are constant and independent of R_T and *Le* and the boundary layer thickness is

monotonically decreasing with Le. However, for given $N > -1$, the results obtained for the heat and mass transfer rates at large Le are depending on R_T and may be dominated by convection if R_T is large enough. For this case, the boundary layer thicknesses present an asymptotic evolution with Le. Finally, the existence of a particular boundary layer regime has been predicted in this study for the particular case where $N + Le^2 = 0$. For this situation, $\Omega \sim R_T^{4/9}$, $Nu \sim R_T^{2/9}$ and $Sh \sim R_T^{2/9}$.

References

[1] D.A. Nield, A. Bejan, Convection in Porous Media, Springer Verlag, 1992.

[2] M.C. Charrier-Mojtabi, M. Karimi-Fard, M. Azaiez, A. Mojtabi, Onset of a double-diffusive convection regime in a rectangular porous cavity, J. Porous Media 1 (1998) 107–121.

[3] M. Mamou, P. Vasseur, E. Bilgen, A Galerkin finite-elememt study of the onset of double-diffusive convection in an inclined porous enclosure, Int. J. Heat Mass Transfer 41 (1998) 1513–1529.

[4] M. Mamou, P. Vasseur, E. Bilgen, Double-diffusive convection instability problem in a vertical porous enclosure, J. Fluid Mech 368 (1998) 263–289.

[5] A. Amahmid, M. Hasnaoui, P. Vasseur, Etude analytique et numérique de la convection naturelle dans une couche poreuse de Brinkman doublement diffusive, Int. J. Heat Mass Transfer 42 (1999) 2991–3005.

[6] O.V. Trevisan, A. Bejan, Natural convection with combined heat and mass transfer buoyancy effects in a porous medium, Int. J. Heat Mass Transfer 28 (1985) 1597–1611.

[7] D.K. Lin, Unsteady natural convection heat and mass transfer in a saturated porous enclosure, Waerme- und Stoffuebertragung 28 (1993) 49–56.

[8] F. Alavyoon, Y. Masuda, S. Kimura, On natural convection in vertical porous enclosures due to opposing fluxes of heat and mass prescribed at the vertical walls, Int. J. Heat Mass Transfer 37 (1994) 195–206.

[9] M. Mamou, P. Vasseur, E. Bilgen, D. Gobin, Double-diffusive convection in an inclined slot filled with porous medium, European J. of Mechanics B/Fluids 14 (1995) 629–652.

[10] P. Nithirasu, K.N. Seetharamu, T. Sundararajan, Double-diffusive natural convection in an enclosure filled with fluid-saturated porous medium: a generalized non-Darcy approach, Num. Heat Transfer, Part A 30 (1996) 413–426.

[11] M. Mamou, P. Vasseur, E. Bilgen, Multiple solutions for double-diffusive convection in a vertical porous enclosure, Int. J. Heat Mass Transfer 38 (1995) 1787–1798.

[12] A. Amahmid, M. Hasnaoui, M. Mamou, P. Vasseur, On the transition between aiding and opposing double diffusive flows in a vertical porous matrix, J. Porous Media, submitted.

[13] O.V. Trevisan, A. Bejan, Mass and heat transfer by natural convection in a vertical slot filled with porous medium, Int. J. Heat Mass Transfer 29 (1986) 403–415.

[14] F. Alavyoon, On natural convection in vertical porous enclosures due to prescribed fluxes of heat and mass at the vertical boundaries, Int. J. Heat Mass Transfer 36 (1993) 2479–2498.

[15] P. Roache, Computational Fluid Dynamics, Hermosa, Albuquerque, NM, 1982.